Accepted version of Manuscript submitted to *Nature Astronomy*

Rare meteorites common in the Ordovician period

Philipp R. Heck[1,2], Birger Schmitz[1,3], William F. Bottke[4], Surya S. Rout[1,2], Noriko T. Kita[5], Anders Cronholm[3], Céline Defouilloy[5], Andrei Dronov[6,7] & Fredrik Terfelt[3]

[1]Robert A. Pritzker Center for Meteoritics and Polar Studies, The Field Museum of Natural History, 1400 South Lake Shore Drive, Chicago, IL 60605, USA.
[2]Chicago Center for Cosmochemistry and Department of the Geophysical Sciences, The University of Chicago, 5734 South Ellis Avenue, Chicago, IL 60637, USA.
[3]Astrogeobiology Laboratory, Department of Physics, Lund University, P.O. Box 118, SE-22100 Lund, Sweden.
[4]Department of Space Studies, Southwest Research Institute, 1050 Walnut St, Suite 300, Boulder, CO 80302, USA.
[5]WiscSIMS, Department of Geoscience, University of Wisconsin-Madison, 1215 W. Dayton Street, Madison, WI 53706-1692, USA.
[6]Geological Institute, Russian Academy of Sciences, Pyzhevsky per.7, 119017 Moscow, Russia.
[7]Kazan (Volga Region) Federal University, Kremlevskaya ul. 18, 420008 Kazan, Russia.

Most meteorites that fall today are H and L type ordinary chondrites, yet the main belt asteroids best positioned to deliver meteorites are LL chondrites[1,2]. This suggests the current meteorite flux is dominated by fragments from recent asteroid breakup events[3,4] and therefore is not representative over longer, e.g. 100 Myr, timescales. Here we present the first reconstruction of the composition of the background meteorite flux to Earth on such time scales. From limestone that formed about one million years before the breakup of the L-chondrite parent body 466 Myr ago, we have recovered relict minerals from coarse micrometeorites. By elemental and oxygen-isotopic analyses we show that before 466 Myr ago achondrites from different asteroidal sources were in similar or higher abundances than ordinary chondrites. The primitive achondrites, such as lodranites and acapulcoites, together with related ungrouped achondrites, made up ~15-34% of the flux compared to only ~0.45% today. Another group of abundant achondrites may be linked to a 500 km cratering event on (4) Vesta that filled the inner main belt with basaltic fragments a billion years ago[5]. Our data show that the meteorite flux has varied over geological time as asteroid disruptions create new fragment populations that then slowly fade away from collisional and dynamical evolution. The current flux favors disruption events that are larger, younger, and/or highly efficient at delivering material to Earth.

In order to investigate the past meteorite flux, we searched for relict chrome-spinel grains of coarse micrometeorites in condensed marine sediments in northwestern Russia in a ~10-100 kyr time window in the geological epoch of the Middle Ordovician which ranges from 470 to 458 Myr (Fig. 1; see Methods). Chrome spinels are the only minerals of meteorites and coarse micrometeorites that survived diagenesis in Ordovician limestone[6]. They retained their elemental and oxygen isotopic composition, enabling reliable classification based on single grain microanalysis[7,8]. We also dissolved 32 meteorites of different types in HF or HCl acid in order to quantify their content of chrome-spinel grains. Our sediment sample studied is about one million years older than the ~466 Myr old sediments that contain the first collisional fragments from the L-chondrite parent body breakup (LCPB), the largest known asteroid disruption event in the last three billion years. The sampling level was chosen in order to exclude the extreme flux enhancement (more than two orders of magnitude[6,7]) of L-chondritic fragments after the LCPB that obscures the background flux for more than 1 Myr[7–9]. The low, 50 to 100 kyr, cosmic-ray exposure ages of the oldest recovered fossil L chondrites[9] indicate that a sample separation of one million years before the strata containing the first abundant L chondrites is large enough to assess the pre-LCPB flux. The interval sampled represents a time average of about 10 to 100 kyr and was selected with the aim to determine if the composition of the meteorite flux to Earth was similar or different to what it is today. This is the first reconstruction of the background flux of the different meteorite types in a geological time perspective. Similar reconstructions are ongoing for other periods in Earth's geological past[10].

The presence of surface-implanted solar wind-derived helium and neon in sediment-dispersed chrome spinels (SECs) that were recovered from similar sediments from several younger Ordovician beds from sites in Sweden, China and Russia is evidence that the SECs were parts of coarse micrometeorites[11–13]. Because the abundance ratio of the two ordinary chondrite groups H and L chondrites in recently fallen coarse micrometeorites[14,15] is similar to this ratio in macroscopic meteorites, micrometeorites bearing coarse chromite grains can be used as a proxy for meteorites[7]. The same consistency between the composition of coarse micrometeorites and meteorites has been documented based on fossil material for the Ordovician period after the LCPB[8]. This relation is useful because of the much higher abundance of SECs compared to fossil meteorites[6] that allows analyses of a larger number of samples[7].

We recovered 46 chrome-spinel grains with diameters >63 μm out of which 41 of them are extraterrestrial based on their oxygen isotopic and elemental composition (Table 1 and Supplementary Data 1; Methods). We find a large diversity of micrometeorites that includes all three groups of ordinary chondrites and many types of achondrites in strikingly different proportions than today (Figs. 2 and 3). Among the extraterrestrial grains 23 originate from ordinary chondrites and 18 from achondrites. This corresponds to an ordinary chondrite/achondrite ratio of 1.3 compared to ~11 in today’s flux (Table 1). The proportions of the three ordinary chondrite groups H, L, and LL are markedly different compared to the recent flux, and to the flux immediately after the LCPB. Today L and H chondrites fall in about equal proportions and together dominate the flux, but in the Ordovician prior to the LCPB the same can instead be said about the LL and L types (Table 1).

Considering the variation in abundances of large Cr spinel grains in recent meteorites there are significant uncertainties when translating SEC grain abundances into Middle Ordovician meteorite flux estimates (see Supplementary Data 2). Some first-order minimum estimates for the achondritic versus ordinary chondritic flux can be made, however, if we assume that the achondrites generally held lower or maximally similar chrome-spinel grain contents as the ordinary chondritic (mostly types 5 and 6) micrometeorites that contributed chrome-spinel grains to the ancient sea floor. With this extremely conservative approach the achondrites were almost or as common as the ordinary chondrites, and the primitive achondrites and related ungrouped achondrites made up between 15 and 34% of all achondrites and ordinary chondrites, compared to ca. 0.45% today (Table 1 and Supplementary Information). The true achondrite fraction, however, may have been even significantly higher. Although we have only studied 13 achondrites our data for the abundance of chrome-spinel content indicates generally lower numbers than for the ordinary chondrites. If these numbers are accounted for in the paleoflux estimates achondrites dominated over ordinary chondrites.

The achondrite grains include one sample possibly from a rare Bocaiuva-type achondrite (category A; Figs. 2&3). Based on the elemental and $\Delta^{17}O$ composition of Bocaiuva[16,17] and our category A grain we argue that the grain may represent a piece of the missing mantle fraction of the Bocaiuva parent body, or, of the surface if the Bocaiuva iron was impact-generated. One of our chrome-spinel grains (#105-05) appears to come from the Österplana 065 type of ungrouped achondrite. In Middle Ordovician sediments that formed after the LCPB recently a fossil 8 cm large achondrite, Österplana 065, was found, having a Cr and O isotopic composition different from all known recent meteorite types[18]. This single find of a new type of achondrite among ca. 100 fossil L-chondritic meteorites indicates that our assemblage of micrometeoritic chrome spinel in the present study may also harbor grains from meteorites not known today. If one would make a random find of a single meteorite on Earth today, the likelihood is much higher that it would belong to a common than a very rare group of meteorites. Based on this reasoning, it is likely that Österplana 065 belongs to a type of meteorite that was common in the flux in the Ordovician. The data in this study support that this was the case. For Österplana 065 we know that its chrome-spinel content was rather low, 50 grains per gram. If we use this number in the paleoflux estimates, this would mean that meteorites of the type represented by grain #105-05 alone would represent 20-30 times the mass to which one of the ordinary chondritic grains corresponds to. The unexpected high fraction of ungrouped and related primitive achondritic material in sediments predating the LCPB is evidence that some partially differentiated asteroids had disrupted and were capable of producing a relatively high flux of meteoroids at that time. The fact that the same fraction is smaller today likely indicates their source families were small enough that meteoroid production by a collisional cascade could not keep up with newer families much closer to their peak flux.

As regards howardites, eucrites and diogenites (HED) achondrites, today the HED/ordinary chondrites ratio is ca. 0.1. With a range of 4-12 possible HED micrometeorites among our 41 extraterrestrial grains (of which 23 are ordinary chondritic) this represents a (grain-to-grain) HED/ordinary chondrites ratio in the range 0.2 to 0.5, which is significantly higher than today. Considering also that the HED meteorites on average contain fewer Cr-spinel grains in the >63 μm fraction than the equilibrated ordinary chondrites dominated by higher petrographic types (Supplementary Data 2), this gives additional support for HED meteorites being more abundant in the Middle Ordovician than today. This result is particularly interesting because the HEDs are believed to come from the Vesta family[19] that formed nearly 1 Gyr ago via the formation of the ~500 km Rheasilvia impact basin[5]. The collisional cascade for this family would have been just as capable, if not more so, at producing meteoroids ~467 Myr ago as today.

For our 23 samples with an unambiguously ordinary chondritic origin the most significant difference compared to the recent flux composition is the high abundance of LL grains relative to H and L grains compared to post-LCPB and today (Table 1). Impact degassing ages of recent LL chondrite falls are sparse[20,21] and the only degassing age that could date the same event is that of the Morokweng meteorite (625±163 Ma; ref. 22), others are mostly at or older than 1 Gyr, consistent with the dynamical age of the Flora asteroid family (950 +200/–170 Myr; ref. 23), a likely source of the LL chondrites[2]. The H chondrites in Earth's recent flux have impact degassing ages in the range ca. 280-460 Myr, indicating one or a few younger events than the LCPB 466 Myr ago[21]. This could suggest that the primary source of today's H chondrites had not yet disrupted, while the LL source had disrupted and was closer to its peak meteoroid flux than it is now.

The smaller size fraction (<100 μm) of today's micrometeorites is dominated by carbonaceous chondritic material, reflecting the brittleness and fragmentation of such material upon collision with Earth's atmosphere[24]. In the recent flux the coarse micrometeorites that can contain 100-μm-sized unmelted spinel grans are dominated by ordinary chondritic material similar to the macrometeorite flux composition[24,25]. All previous studies on micrometeorites show that recent primitive achondrite-type micrometeorites are not a significant fraction of the present flux.

The large diversity in our sample of coarse micrometeorites, representing many different types and origins, confirms that the studied sediments did not sample one event such as an atmospheric breakup, terrestrial impact or even a breakup of a single type of asteroid in space, but rather represents a time-averaged sample of the extraterrestrial flux to Earth over ~10-100 kyr. We predict that the same diversity and abundances of coarse micrometeorites should be preserved in sediments of the same age globally.

Despite many uncertainties, using a conservative approach we show for the first time that the meteorite flux composition was fundamentally different ~467 Myr ago than today and varies on timescales of 10-100 Myr and larger. At that time achondrites probably dominated over ordinary chondrites, and primitive achondrites and related ungrouped meteorites were at the least one order, and probably two orders of magnitude more abundant than today. This fits with the scenario that different asteroid families were dominating the meteorite flux at these times. Furthermore, it shows that only after the LCPB L chondrites became the most significant type of coarse extraterrestrial matter that accreted to Earth. These results confirm that the collisional cascade model of meteoroid delivery is reasonable and can help tell us about the evolution of the asteroid belt. Studying different time windows will provide further knowledge about the variation of the flux of extraterrestrial material to Earth in deep time and will provide new knowledge on the evolution of the asteroid belt from Earth's sedimentary record[10].

References

1. Vernazza, P. *et al.* Compositional differences between meteorites and near-Earth asteroids. *Nature* **454**, 858–860 (2008).
2. Dunn, T. L., Burbine, T. H., Bottke, W. F. Jr. & Clark, J. P. Mineralogies and source regions of near-Earth asteroids. *Icarus* **222**, 273–282 (2014).

3. Nesvorný, D., Vokrouhlický, D., Morbidelli, A. & Bottke, W. F. Asteroidal source of L chondrite meteorites. *Icarus* **200**, 698–701 (2009).
4. Bottke, W. F. *et al.* The collisional evolution of the main asteroid belt. In *Asteroids IV* (eds Michel, P. et al.), 701–724 (Univ. Arizona Press, Tucson, 2015).
5. Marchi, S. *et al.* High-velocity collisions from the lunar cataclysm recorded in asteroidal meteorites. *Nat. Geosci.* **6,** 303–307 (2013).
6. Schmitz, B., Häggström, T. & Tassinari, M. Sediment-dispersed extraterrestrial chromite traces a major asteroid disruption event. *Science* **300**, 961–964 (2003).
7. Heck, P.R. *et al.* A search for H-chondritic chromite grains in sediments that formed immediately after the breakup of the L-chondrite parent body 470 Ma ago. *Geochim. Cosmochim. Acta* **177**, 120–129 (2016).
8. Heck, P.R. *et al.* A single asteroidal source for extraterrestrial Ordovician chromite grains from Sweden and China: High-precision oxygen three-isotope SIMS analysis. *Geochim. Cosmochim. Acta* **74**, 497–509 (2010).
9. Heck, P.R., Schmitz, B., Baur, H., Halliday, A. N. & Wieler, R. Fast delivery of meteorites to Earth after a major asteroid collision. *Nature* **430**, 323-325 (2004).
10. Schmitz, B. Extraterrestrial spinels and the astronomical perspective on Earth's geological record and evolution of life. *Chem. Erde* **73**, 117–145 (2013).
11. Heck, P. R., Schmitz, B., Baur, H. & Wieler, R. Noble gases in fossil micrometeorites and meteorites from 470 Myr old sediments from southern Sweden, and new evidence for the L-chondrite parent body breakup event. *Meteorit. Planet. Sci.* **43**, 517–528 (2008).
12. Alwmark, C., Schmitz, B., Meier, M. M. M., Baur, H. & Wieler, R. A global rain of micrometeorites following breakup of the L-chondrite parent body—Evidence from solar wind-implanted Ne in fossil extraterrestrial chromite grains from China. *Meteorit. Planet. Sci.* **47**, 1297–1304 (2012).
13. Meier, M. M. M., Schmitz, B., Lindskog, A., Maden, C. & Wieler, R. Cosmic-ray exposure ages of fossil micrometeorites from mid-Ordovician sediments at Lynna River, Russia. *Geochim. Cosmochim. Acta* **125**, 338–350 (2014).
14. Van Ginneken, M., Folco, L., Cordier, C. & Rochette, P. Chondritic micrometeorites from the Transantarctic Mountains. *Meteorit. Planet. Sci.* **47**, 228–247 (2012).
15. Prasad, M. S., Rudraswami, N. G., De Araujo, A., Babu, E. V. S. S. K. & Kumar, T. V. Ordinary chondritic micrometeorites from the Indian Ocean. *Meteorit. Planet. Sci.* **50**, 1013–1031 (2015).
16. Desnoyers, C. *et al.* Mineralogy of the Bocaiuva iron meteorite: A preliminary study. *Meteoritics* **20**, 113–124 (1985).
17. Clayton, R. N. & Mayeda, T. K. Oxygen isotope studies of achondrites. *Geochim. Cosmochim. Acta* **60**, 1999–2017 (1996).
18. Schmitz, B. *et al.* A new type of solar-system material recovered from Ordovician marine limestone. *Nat. Comm.* **7**, 11851 (2016).
19. Mittlefehldt, D. W. Asteroid (4) Vesta: I. The howardite-eucrite-diogenite (HED) clan of meteorites. *Chem. Erde* **75**, 155–183 (2015).
20. Bogard, D. D. K–Ar ages of meteorites: Clues to parent-body thermal histories. *Chem. Erde* **71**, 207–226 (2011).

21. Swindle, T. D., Kring, D. A. & Weirich, J. R. In Advances in $^{40}Ar/^{39}Ar$ Dating: from Archaeology to Planetary Sciences (eds Jourdan, F., Mark, D. F. & Verati, C.) **378**, 333–347 (2014).
22. Jourdan, F., Andreoli, M. A. G., McDonald, I. & Maier, W. D. $^{40}Ar/^{39}Ar$ thermochronology of the fossil LL6-chondrite from the Morokweng crater, South Africa. *Geochim. Cosmochim. Acta* **74**, 1734 –1747 (2010).
23. Dykhuis, M. J., Molnar, L., Van Kooten, S. J. & Greenberg, R. Defining the Flora Family: Orbital properties, reflectance properties and age. *Icarus* **243**, 111–128 (2014).
24. Cordier, C. & Folco, L. Oxygen isotopes in cosmic spherules and the composition of the near Earth interplanetary dust complex. *Geochim. Cosmochim. Acta* **146**, 18–26 (2014).
25. Suavet, C. *et al.* Ordinary chondrite-related giant (>800 μm) cosmic spherules from the Transantarctic Mountains, Antarctica. *Geochim. Cosmochim. Acta* **75**, 6200–6210 (2011).
26. Cordier, C. *et al.* HED-like cosmic spherules from the Transantarctic Mountains, Antarctica: Major and trace element abundances and oxygen isotopic compositions. *Geochim. Cosmochim. Acta* **77**, 515–529 (2012).

Acknowledgements The study was supported by an ERC-Advanced Grant (ASTROGEOBIOSPHERE) to B.S. We thank K. Deppert and P. Eriksson for support at Lund University, F. Iqbal for the laboratory work, and B. Strack for maintenance of the Field Museum's SEM laboratory. P.R.H. acknowledges funding from the Tawani Foundation. WiscSIMS is partly supported by NSF (EAR03-19230, EAR13-55590). We thank J. Kern for SIMS support. 3D microscopy was performed in the Keck-II facility of the Northwestern University NUANCE Center, supported by NSEC (NSF EEC–0647560), MRSEC (NSF DMR-1121262), the Keck Foundation, the State of Illinois, and Northwestern University. A.D. acknowledges support from Russian Governmental Program of Competitive Growth of Kazan Federal University and RFBR (Grant 16-05-00799). W.F.B's participation was supported by NASA's SSERVI program "Institute for the Science of Exploration Targets (ISET)" through institute grant number NNA14AB03A. We thank the three reviewers who provided helpful comments that improved the manuscript.

Author Contributions P.R.H. and B.S. conceived the study and wrote the paper with input from all authors. W.F.B. provided expertise on the collisional and dynamical evolution of the asteroid belt and meteoroid delivery models. B.S., F.T. and A.D. conducted the fieldwork, B.S., F.T. and A.C. extracted and prepared the samples for SEM/EDS and SIMS. A.C. performed the quantitative SEM/EDS analysis. P.R.H. and S.S.R. prepared the samples for SIMS and performed the SIMS and post-SIMS analyses. N.T.K. and C.D. set up SIMS analysis conditions and assisted with the analyses.

Author Information Reprints and permissions information is available at www.nature.com/reprints. The authors declare no competing financial interests.

Correspondence and requests for materials should be addressed to P.R.H. (prheck@fieldmuseum.org).

Main figure legends

Fig. 1. **Micrometeorite-bearing limestone beds at the Lynna river section in northwestern Russia that were deposited around 466 million years ago.** The sample GAP7 was collected over an interval of highly condensed limestone about 4 m below the level where the first SEC grains that clearly originate from the LCPB have been found. The abundance of all Cr-spinel grains with radius >63 μm retrieved from the GAP7 sample is shown (open square), the solid circles are grains from equilibrated ordinary chondritic micrometeorites. The sizes of the GAP1, GAP2 and GAP6 samples searched for SEC grains were 14, 12 and 13 kg large, respectively. Asterisks symbols after the sample's name indicate the samples studied by ref. 27 and & symbols those studied by ref. 7.

Fig. 2. **Values of $\Delta^{17}O$ and TiO_2 of our data compared to compositions of different relevant meteorite groups.** Reference data compilation is provided in Supplementary Data 3. Grains 105-07, 106-11, and 106-18 fall outside the range shown in this figure (see Supplementary Data 1).

Fig. 3. **Probability density functions (PDFs) of $\Delta^{17}O$ values showing the distribution of different micrometeorite categories.** Top panel: PDFs from data of individual chrome-spinel grains analyzed in this study labeled with the categories A-F as defined in the text and the clearly resolved ordinary chondrite groups (H, L, and LL). Bottom panel: Sums of all PDFs from data from this study compared with data from a previous study[7] of post-LCPB chrome-spinel grains. The post-LCPB flux was dominated by L-chondritic material from the asteroid breakup and obscures the background flux.

Methods

For this study we dissolved 270 kilogram of rock from the interval at and just below the so called *Trypanites* bed in the Lynna River section in the St. Petersburg region of Russia. The studied Lynna River section has been the focus during the past century of many studies of the paleontological and sedimentological record (ref. 27, and references therein). The studied interval is located about 4.7 m below the base of the Ly1 bed[27] and is characterized by very high densities of burrows of a kind that typically develop on hard ground surfaces on the sea floor during extremely slow rates of sedimentation. The rocks were dissolved in HCl (6 M) and HF (11 M) at room temperature in the Lund University Astrogeobiology Laboratory specially built for separation of extraterrestrial minerals from ancient sediments. After sieving at mesh sizes 32 and 63 μm opaque chrome-spinel grains were identified by picking under the binocular microscope and subsequent qualitative SEM/EDS analysis[6]. Only the >63 μm fraction has been used in the present study. We also dissolved in HF or HCl acid small pieces (0.5 to a few gram) of 32 recent and fossil meteorites in order to quantify variations in the content of chrome-spinel grains >63 μm in different meteorite types. We used grains >63 μm to be able to compare our results directly with previous studies of sediment-dispersed extraterrestrial chrome-spinel grains of the same size fraction and because <63 μm terrestrial chrome spinels become more abundant. Furthermore, we have evidence to link the coarse micrometeorite populations that contain coarse chrome-spinel and meteorite populations that contain coarse chrome-spinel. We observe similar type abundances between the two populations today and in Middle Ordovician post-LCPB sediments[7,8]. Polished epoxy grain mounts with centrally mounted analytical standard UWCr-3 (ref. 8) were prepared. A Bruker white light interferometric 3D microscope at Northwestern University was used to verify that grain-to-epoxy topography was kept below 3 μm (on average 2 μm) after polishing to minimize mass-dependent isotope fractionation effects during SIMS analysis[28]. Major and minor element concentrations of polished grains on carbon-coated mounts where analyzed quantitatively with SEM/EDS. Titanium and vanadium oxide concentrations are most resistant to weathering and are most useful, in conjunction with oxygen isotopes, to classify meteorites[6–8]. Isotopes of $^{16}O^-$, $^{17}O^-$ and $^{18}O^-$ were analyzed with a Cameca IMS-1280 SIMS at the WiscSIMS Laboratory at the University of Wisconsin-Madison with conditions and procedures according to ref. 7,8. This procedure includes analysis and correction for the hydride tailing interference on $^{17}O^-$ and bracketing with our analytical standard UWCr-3. The hydride correction was on average 0.17‰ with only three data points above 0.5‰ and all below 1.0‰ (see Supplementary Figure 1 and Supplementary Data 4). As discussed in ref. 7, a correction below 1.0‰ still yields robust data and no data needed to be rejected. A matrix correction was performed by calculating the Al-Mg-spinel fraction (see Supplementary Data 4) in a two-component mixture of Al-Mg-spinel and $FeCr_2O_4$ end members[8]. We determine parts per thousand deviations from VSMOW as $\delta^{18}O$, $\delta^{17}O$ and from the terrestrial mass-fraction line as $\Delta^{17}O$ ($=\delta^{17}O - 0.52 \times \delta^{18}O$), the latter being the main indicator for an extraterrestrial origin (Supplementary Figure 2). We analyzed a total of 58 spots on 46 sediment-dispersed chromite and chrome-spinel grains (grain size ranging from 63 to ca. 200 μm). Based on post-SIMS SEM imaging of SIMS sputtering craters no data points had to be rejected.

The ordinary chondritic grains can be divided into H, L and LL chondrite groups based on their TiO_2 and $\Delta^{17}O$ content as previously demonstrated[7,8] and as illustrated in Figures 2 and 3, and defined in Supplementary Data 1. There is some overlap in $\Delta^{17}O$ and TiO_2 compositions of L and LL chondrites. However, the distribution of $\Delta^{17}O$ and TiO_2 values clearly shows two different populations with different maxima that correspond to these two different groups of ordinary chondrites. The classification of the achondritic grains is more complex, partly because so few types of achondrites to compare with are known today. We have divided our achondritic grains into five categories (A through E) based on their elemental and oxygen isotopic composition (Supplementary Data 1 and Fig. 3).

Category A consists of one grain with an exceptionally low $\Delta^{17}O$ value of –4.3±0.1‰. Carbonaceous chondrites of the CK group can have similar low $\Delta^{17}O$ values, but large chrome-spinel grains have not been observed in this group and are very rare in almost all other groups of carbonaceous chondrites, ruling out such an origin. There are some exceptionally rare pallasites (e.g. Eagle Station) and iron meteorites (Bocaiuva and NWA 176) that have such low $\Delta^{17}O$ values[17]. Neither pallasites nor iron meteorites contain enough large chrome-spinel grains to make a significant imprint on SEC-based studies like this. Silicate inclusions in Bocaiuva, however, contain chrome-spinel grains with remarkably similar elemental composition[16] as our category A grain (Supplementary Data 1).

The five grains in our category B have low $\Delta^{17}O$ values in the range –2 to –0.5‰. This indicates that the grains originate from primitive achondrites, such as lodranites, acapulcoites or related ungrouped achondrites. The recently recovered fossil achondrite Österplana 065 also falls into this category. This meteorite has a $\Delta^{17}O$ composition of –1.08±0.21‰. One of our grains (#105-05) in category B has an oxygen-isotopic and elemental composition very similar to the chrome spinels of Österplana 065 (Fig. 2). Today, meteorites that would yield chrome spinels analogous to our group B grains are extremely rare.

Our category C contains five grains that have $\Delta^{17}O$ values in the range from –0.5‰ to clearly below the terrestrial fractionation line (TFL) within 2SD, and TiO_2 values <2 wt%. Several recent primitive and ungrouped achondrites, for example, the winonaites and brachinites, fall into the $\Delta^{17}O$ range that defines our category C. However, today two thirds of the achondrites are so called HED meteorites, thought to be excavated crustal material from the basaltic 4 Vesta asteroid or other V-type asteroids[19]. These HED meteorites can also have compositions that fall into the range defined as category C. Considering that we recovered as many as five primitive or related ungrouped achondrite grains (category B) it would be strange if there were not also a few such grains with slightly more positive $\Delta^{17}O$ values than the definition of category B. We therefore argue that also some or several of the category C grains may be from primitive or ungrouped achondrites, but a HED origin cannot be ruled out for some.

Our four grains of category D have $\Delta^{17}O$ values in a similar range as those of category C, but high to very high TiO_2 contents (up to >7 wt%). Such high TiO_2 contents in chrome spinels are typical for HED meteorites and are not observed in primitive and ungrouped achondrites. We note that all the grains in categories C and D have high V_2O_3 contents (>0.5 wt%) which is very rare among terrestrial chrome-spinel grains in Middle Ordovician sediments in Baltoscandia[27,29]. This confirms that the small negative offsets in $\Delta^{17}O$ relative to the TFL are real and not analytical or diagenetic artifacts.

The three grains of category E have $\Delta^{17}O$ values at the TFL but, although there is some uncertainty, we argue that their high V_2O_3 (1.2, 1.0, and 0.5 wt%, respectively) concentrations indicate an extraterrestrial origin. Our category F contains five grains with $\Delta^{17}O$ values at the TFL and low (<0.5 wt%) V_2O_3 concentrations. Probably all the grains in this group are terrestrial, but an extraterrestrial origin cannot be ruled out for some. Achondrites with a terrestrial oxygen isotopic composition could have formed in the terrestrial planet region with terrestrial oxygen isotopic compositions and could have been scattered into the main asteroid belt[30]. A recent example of such an ungrouped achondrite is NWA 5363/5400/6077 (ref. 31). The presence of solar-wind implanted or cosmic-ray produced spallogenic helium and neon would unequivocally determine an extraterrestrial origin for those grains.

The proportions of different types of pre-LCPB grains in the present study cannot be directly translated to flux proportions because the number of chrome-spinel grains in different meteorites varies by orders of magnitude (Supplementary Data 2). Our assemblage of grains is most likely representative mainly of the types of meteorites that are rich in large chrome-spinel grains. Therefore we can ignore potential contributions from meteorites that are very low in large chrome spinels, such as the carbonaceous and enstatite chondrites, iron meteorites, pallasites, angrites, aubrites and most ureilites. An ordinary chondrite of petrologic type 5 or 6 can typically contain around 1000-1500 chrome-spinel grains >63 μm per gram, whereas the equivalent number for ordinary chondrites of petrologic type 4 is only 50-150 grains per gram. In meteorites of higher petrologic types chrome-spinel grains are generally also larger with higher degree of equilibration. In the recent flux of ordinary chondrites types 5 and 6 also clearly dominate over type 4. Most likely the majority of our ordinary chondritic SEC grains originate from the more equilibrated meteorites. Achondritic meteorites show also a wide range in chrome-spinel content, from being completely devoid of chrome spinel, like the winonaite Pontlyfni, up to about 1000-1300 grains per gram, e.g. the ungrouped achondrite NWA 6077 or the brachinite NWA 3151. Howardites and diogenites contain on the order of 600-900 grains per gram. Most primitive achondrites, i.e. acapulcoites, lodranites, winonaites, have intermediate chrome-spinel contents, in the range 200-800 grains per gram. We note that there are other types of meteorites that can be rich in large chrome-spinel grains, such as Martian meteorites, and Rumuruti chondrites but none of our grains have elemental and oxygen isotopic compositions consistent with such origins. Similarly there are some anomalous ureilites like NWA 766 that contain common large chrome-spinel grains, but such grains differ in elemental composition from any of our samples (Supplementary Data 2). Middle Ordovician fossil L chondrites show chromite abundances very similar to recent L chondrites attesting to the refractory nature of this meteorite component (Supplementary Data 2).

The data that support the plots within this paper and other findings of this study are available from the corresponding author upon reasonable request.

Additional references used only in Methods

27. Lindskog, A., Schmitz, B., Cronholm, A. & Dronov, A. A Russian record of a Middle Ordovician meteorite shower: Extraterrestrial chromite at Lynna River, St. Petersburg region. *Meteorit. Planet. Sci.* **47**, 1274–1290 (2012).
28. Kita, N. T., Ushikubo, T., Fu, B. & Valley, J. W. High precision SIMS oxygen isotope analysis and the effect of sample topography. *Chem. Geol.* **264**, 43–57 (2009).
29. Schmitz, B. & Häggström, T. Extraterrestrial chromite in Middle Ordovician marine limestone at Kinnekulle, southern Sweden – traces of a major asteroid breakup event. *Meteorit. Planet. Sci.* **41**, 455–466 (2006).
30. Bottke, W. F., Nesvorny, D., Grimm, E. R., Morbidelli, A. & O'Brien D. P. Iron meteorites as remnants of planetesimals formed in the terrestrial planet region. *Nature* **439**, 821–824 (2006).
31. Burkhardt C. *et al.* NWA 5363/NWA 5400 and the Earth: isotopic twins or just distant cousins? *Lun. Planet. Inst.* **46**, 2732 (2015).

Table 1. Classification of coarse micrometeorites in this study with their fractions of the total flux.

	Coarse micrometeorites with matching compositions	**Fraction of total flux 466 Ma ago[&]**	**Fraction of flux today[#]**
Equilibrated ordinary chondrites	**23**	**≤56%**	**91.6%**
H chondrites	5	12%	37.3%
L chondrites	9	22%	43.0%
LL chondrites	9	22%	10.3%
Achondrites	**18**	**≥44%**	**8.3%**
Primitive and ungrouped achondrites incl. Boucaiuva-type mantle	6-14	≥15% to ≥34%	0.45%
HED achondrites	4-12	≥10% to ≥29%	6.6%

[&]The flux estimate is built on the very conservative approach assuming that achondritic meteorites on average are as rich in large Cr-spinel as the equilibrated ordinary chondrites. Our data on Cr-spinel abundances for 32 meteorites indicate that achondrites generally contain fewer >63 µm Cr-spinel grains than equilibrated ordinary chondrites.
[#]The data concerns fraction of the flux excluding the recent major meteorite groups poor in large Cr-spinel (see Table 2).

Table 2. Present-day meteorite fall statistics.

Classification	Present fall #	Fraction of falls
Ordinary chondrites	**897**	**81%**
H	*367*	*33%*
L	*420*	*38%*
LL	*101*	*9.1%*
Other chondrites (C*, E*, R, K* and ungrouped)	**69**	**6.2%**
Achondrites	**81**	**7.3%**
Primitive	*3*	*0.3%*
HED	*64*	*5.8%*
Ungrouped	*1*	*0.1%*
Other (incl. lunar and martian)	*13*	*1.2%*
Iron*, Pallasites*, Mesosiderites*	**60**	**5.4%**
Total	**1107**	**100%**

* Meteorite types generally without or with very low contents of > 63 µm Cr-spinel grains.

Data from Meteoritical Bulletin Database, Version June 15, 2016, http://www.lpi.usra.edu/meteor/metbull.php

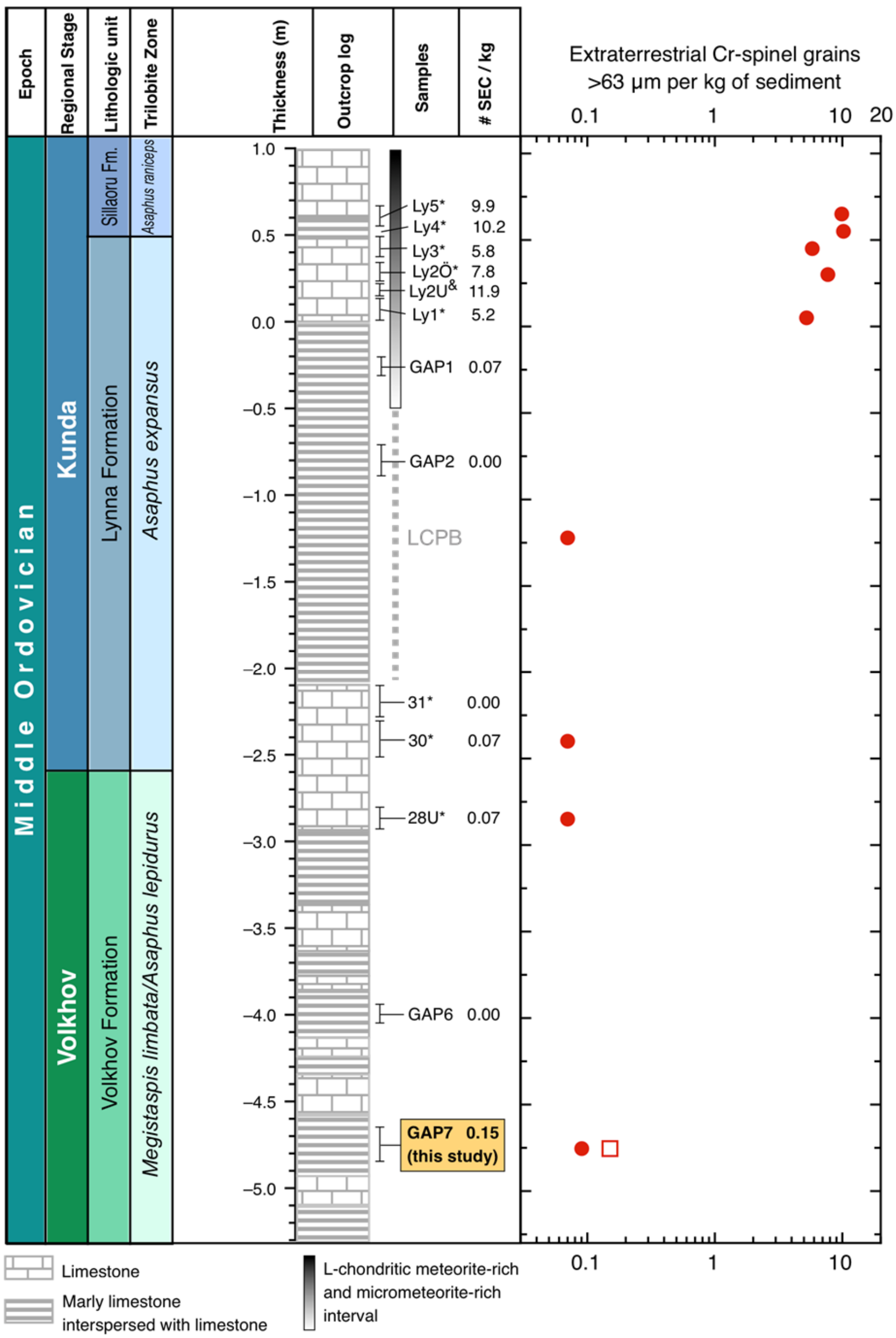

Fig. 1. Micrometeorite-bearing limestone beds at the Lynna river section in northwestern Russia that were deposited around 466 million years ago. The sample GAP7 was collected over an interval of highly condensed limestone about 4 m below the level where the first SEC grains that clearly originate from the LCPB have been found. The abundance of all Cr-spinel grains >63 µm retrieved from the GAP7 sample is shown (open square), the solid circles are grains from equilibrated ordinary chondritic micrometeorites. The sizes of the GAP1, GAP2 and GAP6 samples searched for SEC grains were 14, 12 and 13 kg large, respectively. Intervals sampled by previous studies are labeled (*ref. 8, &ref. 10).

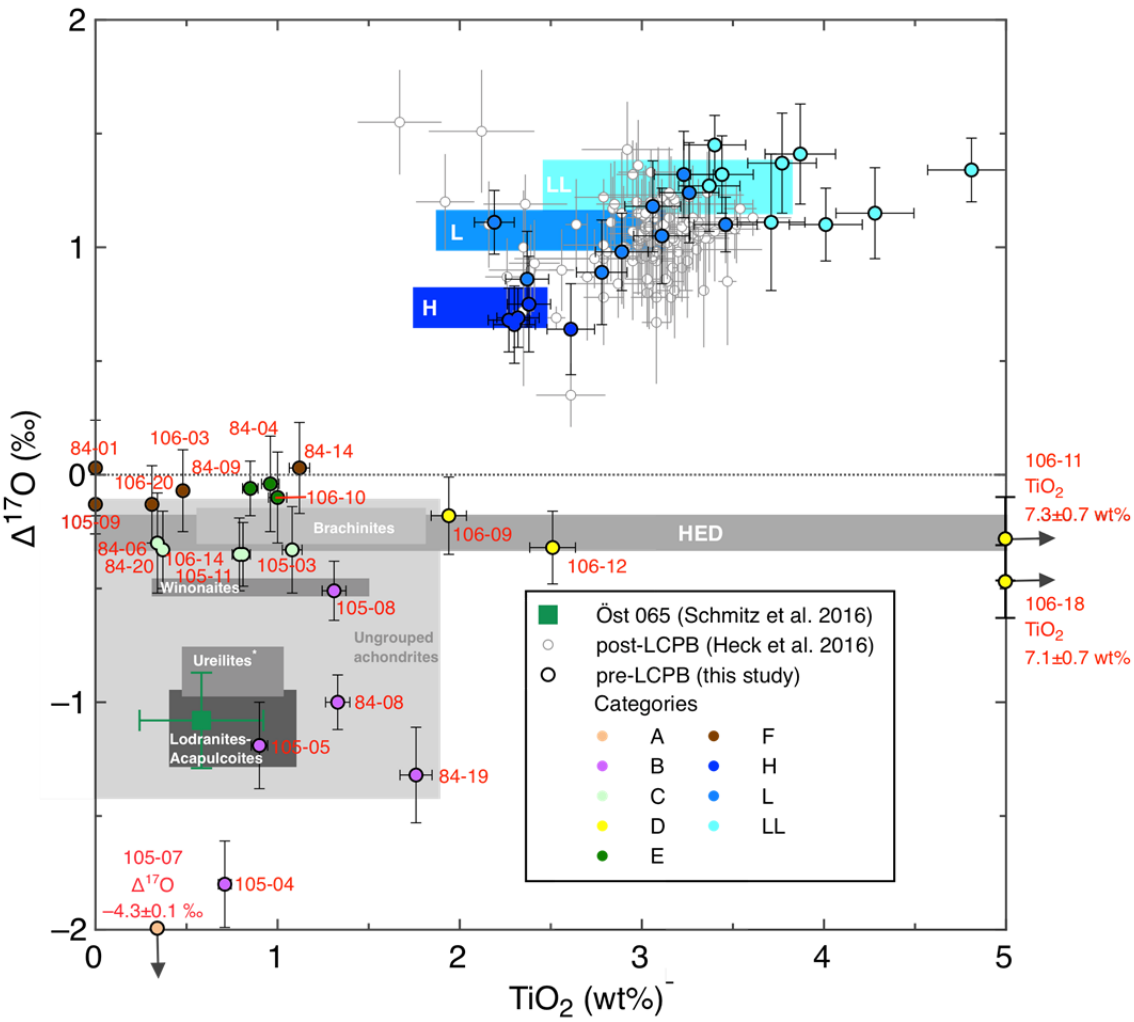

Fig. 2. Values of $\Delta^{17}O$ and TiO_2 of our data compared to compositions of different relevant meteorite groups. Reference data compilation is provided in the supplementary information. Grains 105-07, 106-11, and 106-18 plot outside the range shown in this figure (see Supplementary Table 1).

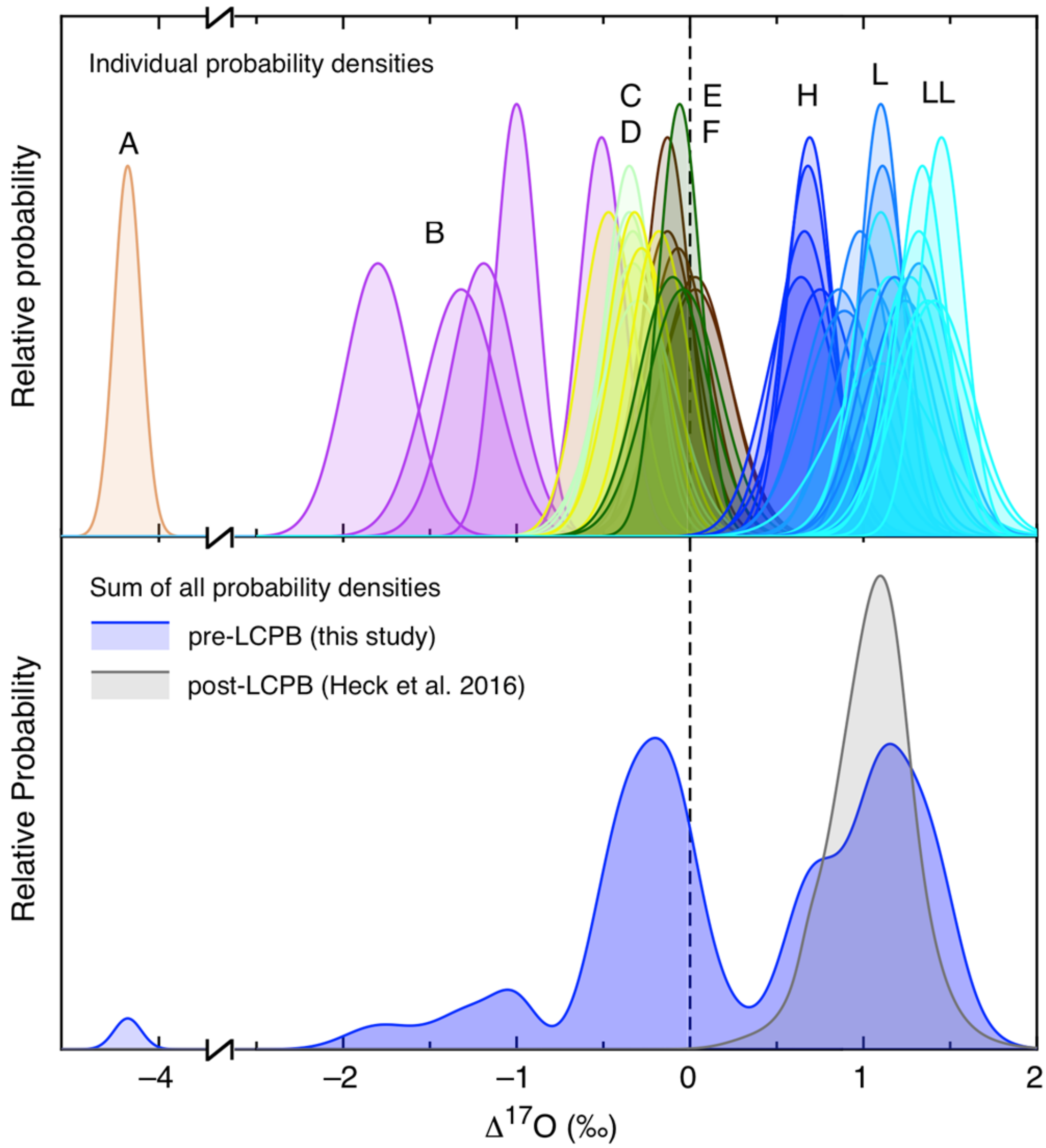

Fig. 3. Top panel: probability density functions (PDFs) of $\Delta^{17}O$ values of individual chrome-spinel grains analyzed in this study labeled with the categories A-F as defined in the text and the clearly resolved ordinary chondrite groups (H, L, and LL). Bottom panel: Sums of all PDFs from data from this study compared with data from a previous study[10] of post-LCPB chrome-spinel grains. The post-LCPB flux was dominated by L-chondritic material from the asteroid breakup and obscures the background flux.

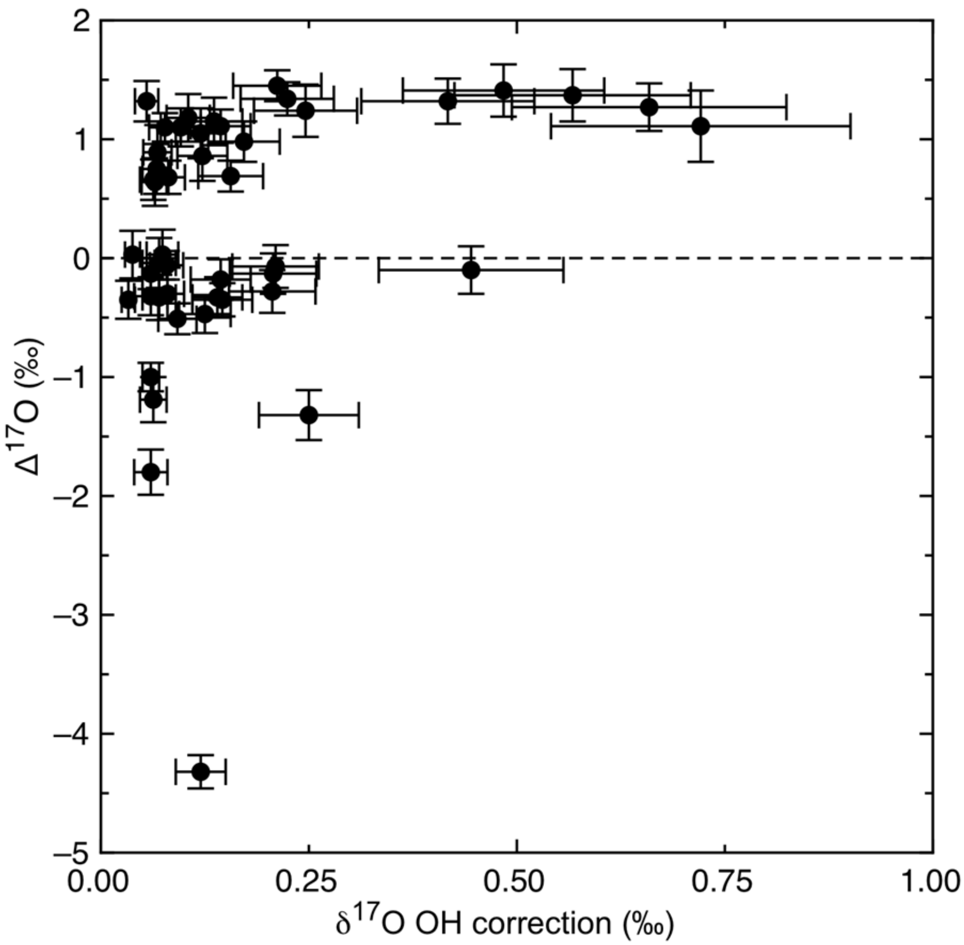

Supplementary Fig. 1. Values of $\Delta^{17}O$ shown with corresponding $[^{16}O^{1}H]^{-}$ correction on $\delta^{17}O$. Error bars are 2σ.

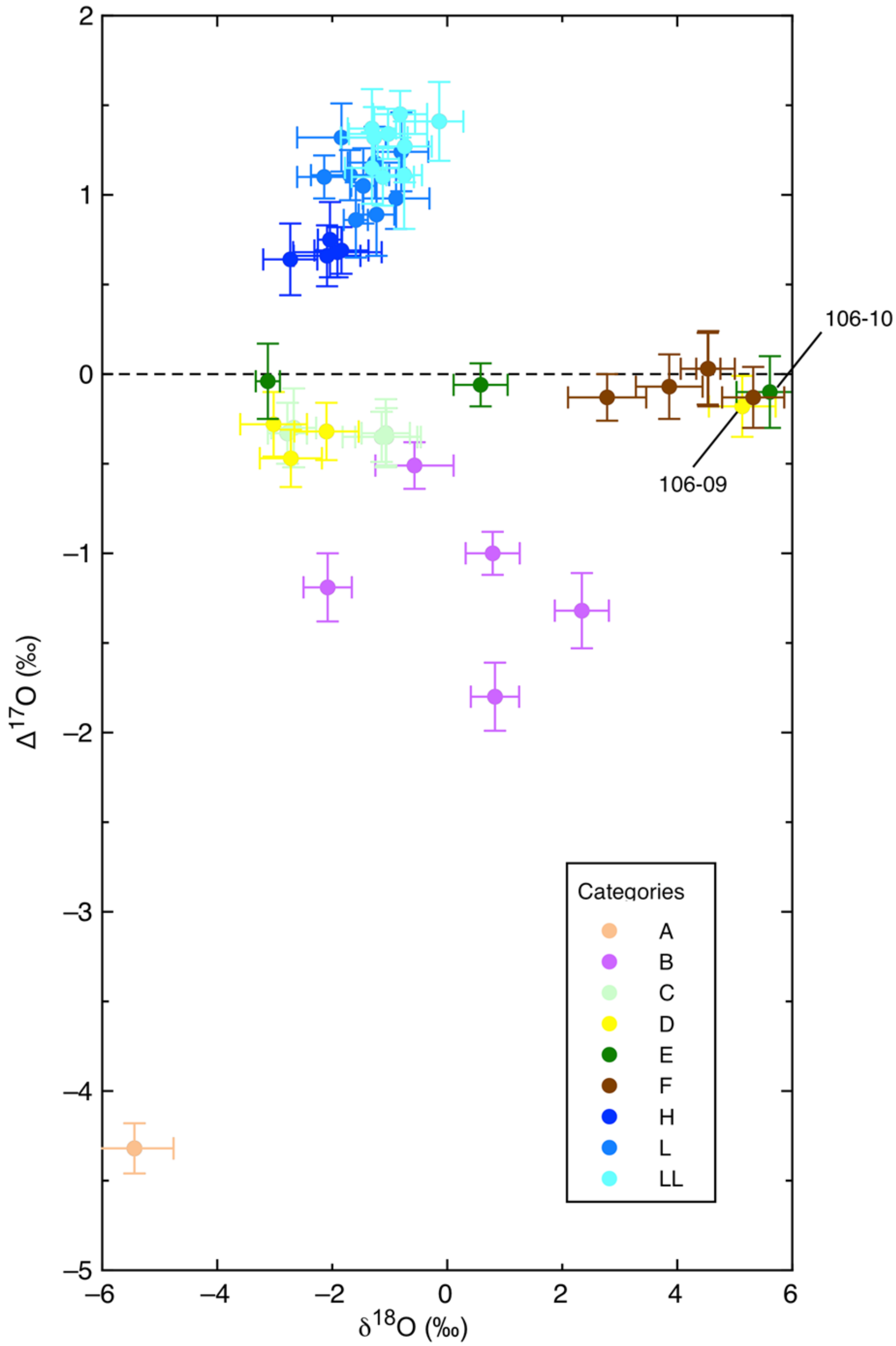

Supplementary Fig. 2. Values of of $\Delta^{17}O$ and $\delta^{18}O$. Although samples 106-10 and 106-09 have $\Delta^{17}O$ and $\delta^{18}O$ values similar to group F grains they have high V_2O_3 contents (1.2 and 0.5 wt%, resp.) which indicates that are likely extraterrestrial.

Supplementary Table 1. Samples from this study grouped into different categories.

Sample ID	$\Delta^{17}O$	±2SE	TiO_2	V_2O_3	Category	Most likely classification
Group A: Ungrouped achondrite; very low $\Delta^{17}O$, mantle equivalent to Bocaiuva or NWA 176						
105-07	-4.32	0.14	0.34	0.34	A	Bocaiuva-type
Group B: Primitive or ungrouped achondrites, $\Delta^{17}O$ of –2 to –0.5 ‰						
105-04	-1.80	0.19	0.71	0.63	B	Ungrouped achondrite
84-19	-1.32	0.21	1.76	0.57	B	Primite or ungrouped achondrite
105-05	-1.19	0.19	0.9	0.38	B	Primite or ungrouped achondrite
84-08	-1.00	0.12	1.33	0.32	B	Primite or ungrouped achondrite
105-08	-0.51	0.13	1.31	0.62	B	Primite or ungrouped achondrite
Group C: Primitive or ungrouped achondrites or HEDs, $\Delta^{17}O$ from –0.5‰ to clearly below TFL within 2SD, TiO_2 <2 wt%						
105-11	-0.35	0.14	0.81	0.72	C	Primite or ungrouped achondrite, or HED
106-14	-0.35	0.16	0.79	1.09	C	Primite or ungrouped achondrite, or HED
84-06	-0.33	0.17	0.37	0.78	C	Primite or ungrouped achondrite, or HED
105-03	-0.33	0.19	1.08	0.66	C	Primite or ungrouped achondrite, or HED
84-20	-0.30	0.22	0.34	0.83	C	Primite or ungrouped achondrite, or HED
Group D: HEDs, D17O from -0.5‰ to clearly below TFL within 2SD, TiO2 >~2 wt% to >7 wt%						
106-18	-0.47	0.16	7.11	0.72	D	HED
106-12	-0.32	0.16	2.51	0.78	D	HED
106-11	-0.28	0.18	7.31	0.7	D	HED
106-09	-0.18	0.17	1.94	0.48	D	HED
Group E: Primitive or ungrouped achondrites or HEDs, $\Delta^{17}O$ near but still below TFL, but V_20_3 >0.5%						
106-10	-0.10	0.20	1	1.19	E	Primite or ungrouped achondrite, or HED
84-09	-0.06	0.12	0.85	0.46	E	Primite or ungrouped achondrite, or HED
84-04	-0.04	0.21	0.96	0.98	E	Primite or ungrouped achondrite, or HED
Group F: Probably terrestrial, D17O at TFL, V2O3 <0.5%						
106-20	-0.13	0.17	0.31	0	F	Terrestrial
105-09	-0.13	0.13	0.00	0.00	F	Terrestrial
106-03	-0.07	0.18	0.48	0.28	F	Terrestrial

Sample ID	$\Delta^{17}O$	±2SE	TiO_2	V_2O_3	Category	Most likely classification
84-14	0.03	0.20	1.12	0.3	F	Terrestrial
84-01	0.03	0.21	0	0	F	Terrestrial
Group H: $\Delta^{17}O$ <0.75‰, TiO_2 <2.70 wt%						
84-13	0.64	0.20	2.61	0.59	H	Equilibrated H chondritic
106-02	0.66	0.17	2.3	0.78	H	Equilibrated H chondritic
105-12	0.68	0.14	2.27	0.69	H	Equilibrated H chondritic
84-10	0.69	0.13	2.32	0.61	H	Equilibrated H chondritic
84-02	0.75	0.21	2.38	0.69	H	Equilibrated H chondritic
Group L: $\Delta^{17}O$ >0.75‰ and TiO_2 <3.40 wt%						
84-05	0.86	0.21	2.37	0.74	L	Equilibrated L chondritic
84-21	0.89	0.23	2.78	0.77	L	Equilibrated L chondritic
106-07	0.98	0.17	2.89	0.88	L	Equilibrated L chondritic
84-03	1.05	0.21	3.11	0.80	L	Equilibrated L chondritic
84-11*	1.10	0.12	3.46	0.87	L	Equilibrated L chondritic
105-06	1.11	0.14	2.19	0.86	L	Equilibrated L chondritic
84-17	1.18	0.20	3.06	0.77	L	Equilibrated L chondritic
84-16*	1.24	0.22	3.26	0.67	L	Equilibrated L chondritic
105-14*	1.32	0.19	3.23	0.73	L	Equilibrated L chondritic
Group LL: $\Delta^{17}O$ >1.10‰ and TiO_2 >3.40 wt%						
106-15	1.10	0.16	4.01	0.75	LL	Equilibrated LL chondritic
84-22*	1.11	0.30	3.71	0.83	LL	Equilibrated LL chondritic
84-15	1.15	0.20	4.28	0.8	LL	Equilibrated LL chondritic
84-12*	1.27	0.20	3.37	0.82	LL	Equilibrated LL chondritic
106-01	1.32	0.17	3.44	0.67	LL	Equilibrated LL chondritic
105-10	1.34	0.14	4.81	0.81	LL	Equilibrated LL chondritic
105-02	1.37	0.22	3.77	0.72	LL	Equilibrated LL chondritic
105-01	1.41	0.22	3.87	0.76	LL	Equilibrated LL chondritic
84-07	1.45	0.13	3.4	0.7	LL	Equilibrated LL chondritic

*) See references 10 and 13 about classification of ordinary chondritic grains based on $\Delta^{17}O$ and TiO_2 values.

Supplementary Table 2. Abundances of coarse Cr-spinel grains in different types of meteorites.

Meteorite	Classification	Cr-spinels, >63 µm/g	Weight dissolved (g)
Allende	CV3	0	6
Acfer 331	CM2	0	8
Ornans	CO3.4	0.75	4
NWA 801	CR2	0.25	4
NWA 7317	CR6	718	0.5
NWA 2129	CK4	0	4.5
NWA 10411	Howardite	638	2.9
NWA 8365	Eucrite	59	2.4
NWA 10403	Diogenite	896	2.3
NWA 766	Ureilite (Cr-spinel	371	3.1
Winona	Winonaite	216	0.87
NWA 725	Winonaite	880	3.1
NWA 4024	Winonaite	80	1.2
Pontlyfni	Winonaite	0	0.73
NWA 10265	Lodranite	788	1.4
NWA 8287	Acapulcoite	314	1.3
NWA 3151	Brachinite	1258	1.1
NWA 6077	Ungrouped achon	1126	1.4
Seymchan	Pallasite (silicate-p	1	3.7*
Ekeby	H4	120	3
Saratov	L4	73	2.2
Hedeskoga	H5	61	3
SAU 001	L5	79	2.3
Mt. Tazerzait	L5	1231	2.2
Ozona	H6	1236	2.1
Lundsgård	L6	1104	0.55
Alfianello	L6	1628	2.2
Österplana 049	Fossil L	158	0.64
Österplana 056	Fossil L	1542	0.72
Österplana 060	Fossil L	691	0.46
Österplana 064	Fossil L	77	0.62
Österplana 065	Fossil ungr. achondrite	50	1.6

Averages	Mean grains/g	1SD	Relative to EOCs
C chondrites (CV3, CM2, CO3.4, CR2, CK4)	0.2	0.3	0.03%
C chondrites incl. CR6 (CV3, CM2, CO3.4, CR2, CR6, CK4)	119.8	293	18%
HED	531.0	429	80%
Ungrouped and/or primitive achondrites (Win, L-A, Öst 065)	523.6	492	79%
Boucaiuva-type EOCs	666.7	639	100%

Supplementary Table 3. Literature compilation.

Elemental compositions of Cr-spinel grains measured with electron microprobe analysis

Classification	N = # of meteorites	MgO	2SD	Al_2O_3	2SD	TiO_2	2SD	V_2O_3	2SD	Cr_2O_3	2SD	MnO	2SD	FeO	2SD	ZnO	2SD	References
HEDs	86	2.53	1.76	9.28	4.04	4.11	5.60	0.55	0.20	49.71	9.61	0.57	0.10	32.74	6.62	0.01	0.01	1-8
Brachinites	8	4.50	0.55	11.37	2.59	1.19	0.63	0.66	0.12	53.39	2.01	0.36	0.04	28.46	0.81	0.02	0.00	9-11
Lodranites-Acapulcoites	5	7.49	2.86	6.89	1.13	0.76	0.35	0.57	0.11	60.82	1.81	1.47	0.89	19.71	4.78	0.70	0.21	12
Ureilites (chromite-bearing)	5	11.36	4.81	15.33	1.83	0.76	0.28	0.46	0.07	53.92	3.44	0.53	0.23	16.62	7.77	0.37	0.07	13, 14
Winonaites	4	8.04	3.01	10.48	11.13	0.91	0.60	0.55	0.24	56.58	11.83	1.78	0.91	21.46	5.33	0.72	0.96	15, 16
Ungrouped achondrites	3	4.76	0.77	4.25	3.16	0.80	1.10	0.78	0.38	62.52	5.55	0.66	0.28	25.33	2.93	0.00	0.00	17, 18
Bocaiuva	1	9.46	2.18	5.97	5.98	0.74	0.35			63.40	5.09	1.76	0.36	18.70	2.40			19
Öst 065	1	4.53	1.28	24.18	7.86	0.58	0.34	0.53	0.19	42.77	8.56	0.20	0.30	25.65	1.62	0.69	0.29	15
H5-6	19	3.03	0.50	6.28	0.56	2.19	0.36	0.67	0.03	56.84	0.77	0.91	0.11	30.09	1.29	0.41	0.25	20-22
L5-6	12	2.39	0.65	5.48	0.64	2.91	0.34	0.72	0.04	56.01	0.81	0.71	0.14	32.08	1.31	0.33	0.08	20-22
LL5-7	10	1.70	0.26	5.64	0.34	3.28	0.68	0.71	0.07	54.86	0.96	0.59	0.11	33.54	1.65	0.24	0.00	20-22
H4-6	28	3.01	0.45	6.31	0.53	2.12	0.37	0.67	0.04	57.03	0.90	0.90	0.11	30.00	1.24	0.40	0.23	20-22
L4-6	19	2.25	0.59	5.18	0.99	2.50	0.63	0.73	0.05	56.96	1.58	0.71	0.14	32.05	1.17	0.34	0.07	20-22
LL4-7	12	1.70	0.24	5.14	1.43	3.15	0.69	0.72	0.07	55.39	1.62	0.58	0.10	33.74	1.54	0.24		20-22

Oxygen isotopic bulk compositions measured by laser-assisted fluorination mass spectrometry

Classification	N = # of meteorites	$\Delta^{17}O$	2SD	$\delta^{17}O$	2SD	$\delta^{18}O$	2SD	Comments	References
HEDs	10	-0.26	0.08	1.52	0.17	3.41	0.26		23
Angrites	4	-0.15	0.06	1.77	0.12	3.69	0.15		23
Brachinites	10	-0.23	0.08	2.05	0.32	4.35	0.51		24
Lodranites-Acapulcoites	28	-1.12	0.17	0.62	0.37	2.86	1.43		24
Ureilites (chromite-bearing)	3	-0.87	0.11	3.14	0.19	7.70	0.14		23
Winonaites	17	-0.50	0.04	1.94	0.67	4.45	1.76		24
Ungrouped achondrites	5	-0.77	0.66	1.06	1.41	4.00	1.55		24,25
Bocaiuva	1	-4.38		-5.54		-2.21		silicate inclusions	23
Öst 065	1	-1.08	0.21	0.61	0.18	3.25	0.18		26
H5-6	17	0.71	0.09	2.82	0.15	3.99	0.17		27
L5-6	23	1.07	0.11	3.50	0.12	4.67	0.20		27
LL5-7	16	1.25	0.13	3.82	0.16	4.96	0.18		27
H4-6	26	0.73	0.09	2.85	0.15	4.08	0.22		27
L4-6	30	1.07	0.09	3.52	0.14	4.70	0.24		27
LL4-6	23	1.26	0.12	3.88	0.16	5.04	0.24		27

References

1 Arai, T., Takeda, H., Lofgren, G. E., & Miyamoto, M. Metamorphic transformations of opaque minerals in some eucrites. *Antarctic meteorite research* **11,** 71 (1998).
2 Mittlefehldt, D. W. Asteroid (4) Vesta: I. The howardite-eucrite-diogenite (HED) clan of meteorites. *Chem. Erde* **75**, 155-183, (2015).
3 Patzer, A., Schlüter, J., Schultz, L., Hill, D. H. & Boynton, W. V. The new polymict eucrite Dar al Gani 983: Petrography, chemical composition, noble gas record, and evolution. *Meteorit. Planet. Sci.* **40**, 869-879, (2005).
4 Mittlefehldt, D. W. & Lindstrom, M. M. Geochemistry of eucrites: Genesis of basaltic eucrites, and Hf and Ta as petrogenetic indicators for altered Antarctic eucrites. *Geochim. Cosmochim. Acta* **67**, 1911-1934 (2003).
5 Berkley, J. L. & Boynton, N. J. Minor/major element variation within and among diogenite and howardite orthopyroxenite groups. *Meteoritics* **27**, 387-394 (1992).
6 Bowman, L. E., Papike, J. & Spilde, M. N. Diogenites as asteroidal cumulates: Insights from spinel chemistry. *American Mineralogist* **84**, 1020-1026 (1999).
7 Papike, J. J., Shearer, C. K., Spilde, M. N. & Karner, J. M. Metamorphic diogenite Grosvenor Mountains 95555: Mineral chemistry of orthopyroxene and spinel and comparisons to the diogenite suite. *Meteorit. Planet. Sci.* **35**, 875-879 (2000).
8 Barrat, J. A. *et al.* Petrology and geochemistry of the fine grained, unbrecciated diogenite northwest Africa 4215. *Meteorit. Planet. Sci.* **41**, 1045-1057 (2006).
9 Gardner-Vandy, K. G., Lauretta, D. S. & McCoy, T. J. A petrologic, thermodynamic and experimental study of brachinites: Partial melt residues of an R chondrite-like precursor. *Geochim. Cosmochim. Acta* **122**, 36-57 (2013).
10 Mittlefehldt, D. W., Bogard, D. D., Berkley, J. L. & Garrison, D. H. Brachinites: Igneous rocks from a differentiated asteroid. *Meteorit. Planet. Sci.* **38**, 1601-1625 (2003).
11 Goodrich, C. A., Wlotzka, F., Ross, D. K., & Bartoschewitz, R. Northwest Africa 1500: Plagioclase bearing monomict ureilite or ungrouped achondrite? *Meteorit. Planet. Sci.* **41**, 925-952 (2003).
12 Mittlefehldt, D. W., Lindstrom, M. M., Bogard, D. D., Garrison, D. H. & Field, S. W. Acapulco-and Lodran-like achondrites: Petrology, geochemistry, chronology, and origin. *Geochim. Cosmochim. Acta* **60**, 867-882 (1996).
13 Chikami, J., Mikouchi, T., Takeda, H. & Miyamoto, M. Mineralogy and cooling history of the calcium aluminum chromium enriched ureilite, Lewis Cliff 88774. *Meteorit. Planet. Sci.* **32**, 343-348 (1997).
14 Goodrich, C. A., Harlow, G. E., Van Orman, J. A., Sutton, S. R., Jercinovic, M. J. & Mikouchi, T. Petrology of chromite in ureilites: Deconvolution of primary oxidation states and secondary reduction processes. *Geochim. Cosmochim. Acta* **135**, 126-169 (2014).
15 Schmitz, B. *et al.* A fossil winonaite-like meteorite in Ordovician limestone: A piece of the impactor that broke up the L-chondrite parent body? *Earth Planet. Sci. Lett.* **400**, 145-152 (2014).
16 Bischoff, A. *et al.* Reclassification of Villalbeto de la Peña—Occurrence of a winonaite related fragment in a hydrothermally metamorphosed polymict L chondritic breccia. *Meteorit. Planet. Sci.* **48**, 628-640 (2013).
17 Gardner-Vandy, K. G. *et al.* The Tafassasset primitive achondrite: Insights into initial stages of planetary differentiation. *Geochim. Cosmochim. Acta* **85**, 142-159 (2012).
18 Goodrich, C. A. & Righter, K. Petrology of unique achondrite Queen Alexandra Range 93148: A piece of the pallasite (howardite eucrite diogenite?) parent body? *Meteorit. Planet. Sci.* **35**, 521-535 (2000).
19 Desnoyers, C. *et al.* Mineralogy of the Bocaiuva iron meteorite: A preliminary study. *Meteoritics* **20**, 113-124 (1985).
20 Bunch, T. E., Keil, K. & Snetsinger, K. G. Chromite composition in relation to chemistry and texture of ordinary chondrites. *Geochim. Cosmochim. Acta* 31, 1569-1582 (1967).
21 Snetsinger, K. G., Keil, K. & Bunch, T. E. Chromite from "equilibrated" chondrites. *Am. Mineral.* **52**, 1322–1331 (1967).
22 Wlotzka, F. Cr spinel and chromite as petrogenetic indicators in ordinary chondrites: Equilibration temperatures of petrologic types 3.7 to 6. *Meteorit. Planet. Sci.* **40**, 1673-1702 (2005).
23 Clayton, R. N. & Mayeda, T. K. Oxygen isotope studies of achondrites. *Geochim. Cosmochim. Acta* **60**, 1999-2017 (1996).
24 Greenwood, R. C., Franchi, I. A., Gibson, J. M. & Benedix, G. K. Oxygen isotope variation in primitive achondrites: The influence of primordial, asteroidal and terrestrial processes. *Geochim. Cosmochim. Acta* **94,** 146-163 (2012).
25 Burkhardt C. *et al.* NWA 5363/NWA 5400 and the Earth: isotopic twins or just distant cousins? *Lun. Planet. Inst.* **46**, 2732 (2015).
26 Schmitz, B. *et al.* A new type of solar-system material recovered from Ordovician marine limestone. *Nat. Comm.* **7**, 11851 (2016).
27 Clayton, R. N., Mayeda, T. K., Goswami, J. N. & Olsen, E. J. Oxygen isotope studies of ordinary chondrites. *Geochim. Cosmochim. Acta* **55**, 2317-2337 (1991).

Supplementary Table 4. Full data table with oxygen isotopic compositions measured with SIMS and elemental compositions measured by quantitative EDS.

Sample ID	$\delta^{18}O$	±2SE	$\delta^{17}O$	±2SE	$\Delta^{17}O$	±2SE	$\delta^{17}O_{corr}$	error	MgO	Al_2O_3	TiO_2	V_2O_3	Cr_2O_3	MnO	FeO	ZnO	Total	Al-Mg-spinel fraction
105_gr07	-5.44	0.68	-7.15	0.36	-4.32	0.14	0.12	0.03	5.95	10.93	0.34	0.34	59.12	0.00	23.20	0.23	100.11	0.25
105_gr04	0.83	0.42	-1.37	0.34	-1.80	0.19	0.06	0.02	5.47	16.33	0.71	0.63	51.02	0.53	25.14	0.00	99.84	0.31
84_gr19	2.34	0.47	-0.10	0.47	-1.32	0.21	0.25	0.06	5.22	11.01	1.76	0.57	55.17	0.40	25.44	0.00	99.56	0.24
105_gr05	-2.08	0.42	-2.27	0.34	-1.19	0.19	0.063	0.016	5.36	12.79	0.90	0.38	53.89	1.36	25.19	0.00	99.86	0.27
84_gr08	0.79	0.47	-0.59	0.21	-1.00	0.12	0.06	0.01	11.71	22.13	1.33	0.32	46.51	0.76	18.36	0.00	101.12	0.46
105_gr08	-0.57	0.68	-0.81	0.36	-0.51	0.13	0.092	0.023	5.20	11.59	1.31	0.62	56.96	0.88	24.47	0.00	101.04	0.25
106_gr18	-2.72	0.54	-1.89	0.41	-0.47	0.16	0.125	0.031	2.58	8.02	7.11	0.72	49.77	0.65	31.90	0.00	100.75	0.17
105_gr11	-1.14	0.68	-0.94	0.36	-0.35	0.14	0.146	0.036	5.63	8.13	0.81	0.72	62.00	0.55	22.93	0.00	100.78	0.21
106_gr14	-1.06	0.54	-0.90	0.41	-0.35	0.16	0.033	0.008	4.08	11.24	0.79	1.09	57.64	0.63	25.25	0.00	100.73	0.22
84_gr06	-2.78	0.34	-1.77	0.28	-0.33	0.17	0.14	0.03	3.20	6.82	0.37	0.78	61.82	1.00	26.39	0.51	100.89	0.15
105_gr03	-1.07	0.42	-0.88	0.34	-0.33	0.19	0.07	0.02	3.59	13.29	1.08	0.66	53.16	0.68	27.60	0.00	100.05	0.24
106_gr12	-2.10	0.56	-1.41	0.36	-0.32	0.16	0.06	0.02	2.79	10.13	2.51	0.78	57.62	0.00	26.99	0.00	100.82	0.19
84_gr20	-2.67	0.39	-1.69	0.43	-0.30	0.22	0.08	0.02	3.60	7.77	0.34	0.83	60.60	0.77	25.37	0.67	99.95	0.17
106_gr11	-3.02	0.58	-1.85	0.32	-0.28	0.18	0.206	0.052	1.44	8.11	7.31	0.70	51.15	0.00	31.57	0.00	100.27	0.15
106_gr09	5.13	0.58	2.49	0.32	-0.18	0.17	0.144	0.036	9.48	16.39	1.94	0.48	37.70	0.00	34.38	0.00	100.36	0.33
106_gr20	5.32	0.54	2.64	0.41	-0.13	0.17	0.207	0.052	10.87	29.37	0.31	0.00	39.07	0.00	20.16	0.26	100.04	0.52
105_gr09	2.78	0.68	1.31	0.36	-0.13	0.13	0.06	0.01	8.52	12.93	0.00	0.00	55.39	0.56	22.52	0.00	99.93	0.30
106_gr10	5.61	0.58	2.82	0.32	-0.10	0.20	0.445	0.111	5.92	24.40	1.00	1.19	41.82	0.00	25.21	0.54	100.09	0.41
106_gr03	3.86	0.58	1.94	0.32	-0.07	0.18	0.210	0.052	5.45	24.94	0.48	0.28	31.32	0.00	35.90	0.51	98.88	0.38
84_gr09	0.58	0.47	0.24	0.21	-0.06	0.12	0.079	0.020	5.67	15.40	0.85	0.46	53.16	0.75	24.33	0.00	100.61	0.30
84_gr04	-3.12	0.21	-1.66	0.36	-0.04	0.21	0.07	0.02	6.05	5.74	0.96	0.98	62.66	1.14	22.07	0.00	99.60	0.19
84_gr14	4.53	0.47	2.39	0.47	0.03	0.20	0.038	0.009	15.52	31.97	1.12	0.30	38.84	0.00	13.20	0.00	100.95	0.59
84_gr01	4.54	0.21	2.40	0.36	0.03	0.21	0.074	0.019	11.47	20.05	0.00	0.00	49.38	0.00	18.78	0.00	99.68	0.42
84_gr13	-2.73	0.47	-0.78	0.47	0.64	0.20	0.065	0.016	3.10	6.52	2.61	0.59	59.80	0.99	26.82	0.46	100.89	0.15
106_gr02	-2.09	0.58	-0.43	0.32	0.66	0.17	0.063	0.016	3.42	6.65	2.30	0.78	59.39	1.16	25.79	0.69	100.19	0.16
105_gr12	-1.91	0.77	-0.32	0.45	0.68	0.14	0.081	0.020	6.74	5.83	2.27	0.69	60.30	0.78	23.44	0.00	100.06	0.20
84_gr10	-1.84	0.47	-0.26	0.21	0.69	0.13	0.156	0.039	3.14	6.25	2.32	0.61	59.78	0.89	26.15	0.84	99.98	0.15
84_gr02	-2.04	0.21	-0.31	0.36	0.75	0.21	0.067	0.017	5.29	6.67	2.38	0.69	58.13	0.98	24.58	0.30	99.02	0.19
84_gr05	-1.59	0.21	0.04	0.36	0.86	0.21	0.122	0.030	3.40	6.83	2.37	0.74	57.95	0.92	26.27	0.49	98.97	0.16
84_gr21	-1.23	0.31	0.26	0.39	0.89	0.23	0.068	0.017	6.13	6.37	2.78	0.77	60.00	0.78	23.03	0.43	100.28	0.20
106_gr07	-0.89	0.58	0.51	0.32	0.98	0.17	0.172	0.043	2.01	6.51	2.89	0.88	60.28	0.67	27.95	0.00	101.19	0.13
84_gr03	-1.46	0.21	0.29	0.36	1.05	0.21	0.12	0.03	3.25	5.51	3.11	0.80	59.26	0.93	26.77	0.59	100.22	0.14
84_gr11	-2.14	0.47	-0.02	0.21	1.10	0.12	0.077	0.019	2.55	6.02	3.46	0.87	60.40	0.78	26.02	0.58	100.69	0.14
106_gr15	-1.12	0.54	0.52	0.41	1.10	0.16	0.096	0.024	2.67	5.66	4.01	0.75	58.40	0.54	28.35	0.00	100.39	0.13
84_gr22	-0.75	0.31	0.72	0.39	1.11	0.30	0.721	0.180	3.25	6.29	3.71	0.83	57.77	0.68	26.16	0.65	99.34	0.15
105_gr06	-1.69	0.68	0.24	0.36	1.11	0.14	0.144	0.036	2.85	6.21	2.19	0.86	59.21	0.89	27.35	1.33	100.88	0.14
84_gr15	-1.31	0.47	0.47	0.47	1.15	0.20	0.136	0.034	1.91	5.59	4.28	0.80	57.67	0.89	29.00	0.31	100.46	0.12
84_gr17	-1.26	0.47	0.53	0.47	1.18	0.20	0.105	0.026	2.83	5.23	3.06	0.77	60.04	0.00	28.42	0.76	101.11	0.13
84_gr16	-0.80	0.47	0.82	0.47	1.24	0.22	0.246	0.062	3.77	5.11	3.26	0.67	59.00	1.03	25.26	1.53	99.63	0.15
84_gr12	-0.74	0.47	0.89	0.21	1.27	0.20	0.659	0.165	2.05	6.94	3.37	0.82	56.99	0.71	28.39	0.41	99.68	0.14
105_gr14	-1.84	0.77	0.36	0.45	1.32	0.19	0.417	0.104	2.93	6.53	3.23	0.73	57.36	0.80	27.74	0.38	99.71	0.15
106_gr01	-1.27	0.58	0.66	0.32	1.32	0.17	0.055	0.014	3.23	5.41	3.44	0.67	57.49	0.67	26.94	2.39	100.25	0.14
105_gr10	-1.03	0.68	0.80	0.36	1.34	0.14	0.224	0.056	2.05	5.61	4.81	0.81	58.41	0.65	27.83	0.00	100.16	0.12
105_gr02	-1.31	0.42	0.69	0.34	1.37	0.22	0.567	0.142	1.92	6.01	3.77	0.72	57.97	0.00	30.34	0.00	100.72	0.12
105_gr01	-0.14	0.42	1.34	0.34	1.41	0.22	0.484	0.121	2.29	6.91	3.87	0.76	59.08	0.56	27.25	0.57	101.29	0.14
84_gr07	-0.82	0.47	1.02	0.21	1.45	0.13	0.212	0.053	2.49	6.57	3.40	0.70	56.93	0.74	27.98	0.00	98.81	0.14